

Radio Remnants of Compact Binary Mergers - the Electromagnetic Signal that will follow the Gravitational Waves

Ehud Nakar¹ and Tsvi Piran²

¹ *Raymond and Beverly Sackler School of Physics & Astronomy, Tel Aviv University, Tel Aviv 69978, Israel; udini@wise.tau.ac.il*

² *Racah Institute of Physics, The Hebrew University, Jerusalem 91904, Israel; tsvi@phys.huji.ac.il*

ABSTRACT

The question “what is the observable electromagnetic (EM) signature of a compact binary merger?” is an intriguing one with crucial consequences to the quest for gravitational waves (GW). Compact binary mergers are prime sources of GW, targeted by current and next generation detectors. Numerical simulations have demonstrated that these mergers eject energetic sub-relativistic (or even relativistic) outflows. This is certainly the case if the mergers produce short GRBs, but even if not, significant outflows are expected. The interaction of such outflows with the surround matter inevitably leads to a long lasting radio signal. We calculate the expected signal from these outflows (our calculations are also applicable to short GRB orphan afterglows) and we discuss their detectability. We show that the optimal search for such signal should, conveniently, take place around 1.4 GHz. Realistic estimates of the outflow parameters yield signals of a few hundred μJy , lasting a few weeks, from sources at the detection horizon of advanced GW detectors. Followup radio observations, triggered by GW detection, could reveal the radio remnant even under unfavorable conditions. Upcoming all sky surveys can detect a few dozen, and possibly even thousands, merger remnants at any give time, thereby providing robust merger rate estimates even before the advanced GW detectors become operational. In fact, the radio transient RT 19870422 fits well the overall properties predicted by our model and we suggest that its most probable origin is a compact binary merger radio remnant.

1. Introduction

Compact binary (Neutron star - Neutron star, NS², or Black Hole - Neutron star, BH-NS) mergers are prime sources of gravitational radiation. The GW detectors LIGO (Abbott

et al. 2009a), Virgo (Acernese et al. 2008) and GEO600 (Grote & the LIGO Scientific Collaboration 2008) are designed to optimally detect merger signals. These detectors have been operational intermittently during the last few years reaching their nominal design sensitivity (Abbott et al. 2009b; Sengupta et al. 2010; the LIGO Scientific Collaboration & the Virgo Collaboration 2010) with detection horizons of a few dozen Mpc for NS² and almost a hundred Mpc for BH-NS mergers (the LIGO - Virgo collaboration adopts an optimal canonical distance of 33/70Mpc; Abadie et al. 2010). Both LIGO and Virgo are being upgraded now and by the end of 2015 are expected to be operational at sensitivities $\sim 10 - 15$ times greater than the initial LIGO (Smith & LIGO Scientific Collaboration 2009), reaching a few hundred Mpc detection horizon for NS² mergers and a Gpc for BH-NS mergers (445/927 Mpc are adopted by the LIGO-Virgo collaboration as canonical values; Abadie et al. 2010).

Understanding the observable EM signature of compact binary mergers has several observational implications. First, once the detectors are operational it is likely that the first detection of a GW signal will be around or even below threshold. Detection of an accompanying EM signal will confirm the discovery, thereby increasing significantly the sensitivity of GW detectors (Kochanek & Piran 1993). Second, the physics that can be learned from observations of a merger event through different glasses is much greater than what we can learn through EM or GW observations alone. Finally, even before the detectors are operational, detection of EM signature will enable us to determine the expected rates, a question of outmost importance for the design and the operation policy of the advanced detectors.

The current constraints on the rates are rather loose. The last LIGO and Virgo runs provided only weak upper limits on the merger rates: $8700 \text{ Myr}^{-1} (10^{10} L_{\odot})^{-1}$ corresponding to $\sim 10^5 \text{ yr}^{-1} \text{ Gpc}^{-3}$ for NS² and $4.5 \times 10^4 \text{ Myr}^{-1} (10^{10} L_{\odot})^{-1}$ ($\sim 5 \times 10^5 \text{ Gpc}^{-3} \text{ yr}^{-1}$) for BH-NS (Abbott et al. 2009b). Estimates based on the observed binary pulsars in the Galaxy are highly uncertain, with values ranging from $20 - 2 \times 10^4 \text{ Gpc}^{-3} \text{ yr}^{-1}$ (Phinney 1991; Narayan et al. 1991; Kalogera et al. 2004b,a; Abadie et al. 2010). It has been suggested (Eichler et al. 1989) that short Gamma-Ray Bursts (GRBs) arise from neutron star merger events. The estimated rate of short GRBs are indeed comparable to binary pulsar estimates (Guetta & Piran 2006; Nakar et al. 2006; Guetta & Stella 2009). However, while appealing, the association is not proven yet (Nakar 2007). If correct, the observed rate of short GRBs, $\sim 10 \text{ Gpc}^{-3} \text{ yr}^{-1}$, provides a lower limit to the merger rate. The true rate depends on a poorly constraint beaming angle, resulting in an uncertainty of almost two orders of magnitude. There are no direct estimates of BH-NS mergers, as no such system has ever been observed, and here one has to rely only on a rather model dependent population synthesis (e.g., Belczynski et al. 2008; Mandel & O’Shaughnessy 2010).

Possible EM signals from coalescence events were discussed by several authors. There

are several suggestions (Hansen & Lyutikov 2001; Moortgat & Kuijpers 2004; Pshirkov & Postnov 2010) of a prompt (coinciding with the GW signal) short lived EM signals, mostly in low radio frequencies, whose amplitudes are highly uncertain. Li & Paczyński (1998) suggested that the radioactive decay of ejected debris from the merger will drive a short lived supernova like event. Metzger et al. (2010) calculated the radioactive heating during this process self-consistently. They find that if $0.01M_{\odot}$ is ejected then the optical emission from a merger at 300 Mpc peaks after ~ 1 day at $m_V \approx 24$. If the mass ejection is lower then the optical emission will be even fainter. Finding, and especially identifying the origin of, such rare and faint events in the crowded variable optical sky is an extremely challenging task, even for current and future optical searches like PTF (Law et al. 2009; Rau et al. 2009), PanSTARR, and LSST (LSST Science Collaborations et al. 2009).

An intriguing possibility is that mergers produce short GRBs (Eichler et al. 1989). However, short GRBs are expected to be beamed, and only rarely this EM signal will point towards us. A beamed GRB that is observed off-axis will inevitably produce a long lasting radio “orphan” afterglow (Rhoads 1997; Waxman et al. 1998; Frail et al. 2000; Levinson et al. 2002; Gal-Yam et al. 2006). A key point in estimating the detectability of GRB orphan afterglows is that the well constrained observables are the *isotropic* equivalent energy of the flow and the rate of bursts that point towards earth. However, the detectability of the orphan afterglows depends only on the *total* energy and *true* rate, namely on the poorly constraint jet beaming angle. Levinson et al. (2002) have shown that while large beaming increases the true rate it reduces the total energy, and altogether reduces the detectability of radio orphan afterglows. This counterintuitive result makes the detectability of late emission from a decelerating jet, which produced a GRB when it was still ultra-relativistic, less promising. However, regardless of amount of ultra-relativistic outflow that is launched by compact binary mergers, and of whether they produce short GRBs or not, mergers are most likely do launch an energetic sub-relativistic and mildly-relativistic outflows. The interaction of these outflows with the surrounding matter will inevitably produce blast waves and possibly stronger radio counterparts than that of ultra-relativistic outflows.

Below we first discuss (in §2) the current estimates of mass and energy ejection from compact binary mergers. In §3 we calculate the radio emission resulting from the interaction of this ejecta (sub-relativistic, mildly relativistic and off-axis relativistic) with the surrounding interstellar matter (ISM). The calculations follow to a large extent models of radio Ib/c supernovae¹ (Chevalier 1998; Chevalier & Fransson 2006) and long GRB radio afterglows (Sari et al. 1998; Waxman et al. 1998; Granot & Sari 2002). The success of radio supernova

¹Note that while blast waves from radio SNe propagate into a surrounding wind density profiles the blast wave from a merger is expected to propagate into a constant density surrounding matter.

(SN) modeling, where the observations are superb, indicates that the microphysics is well constrained and that equipartition parameters describe well the physical conditions. Hence the main uncertainty in the predicted radio signal is in the amount of matter ejected from the merger event and its velocity. Luckily the estimates of this important quantity can be significantly improved even using existing numerical models.

We discuss the observational implications for detectability of merger remnants in §4. We estimate the expected rates of detection of different outflows in §4.1. We devote in §4.2 a special attention to short GRB orphan afterglows that are a special case of our model, in which the outflow is launched relativistically, but the radio emission peaks only during its mildly relativistic phase. The estimates of orphan afterglows detectability is independent of whether they are the products of binary mergers or not. In §4.3 we examine possible other radio transients that may hinder the identification of merger remnants. Finally in §4.4 we examine blind transient searches done in the past and we identify RT 19870422 as a possible and even likely merger remnant. We conclude in §5.

2. Mass and energy ejection from compact binary mergers

Numerical simulations of compact binary mergers have been carried out by various groups with two different approaches. Some (e.g., Rosswog et al. 2000; Ruffert & Janka 2001; Rosswog & Price 2007) use Newtonian dynamics (modified to allow for gravitational radiation back-reaction) with detailed microphysics. Others (e.g., Yamamoto et al. 2008; Rezzolla et al. 2010) use full General relativistic dynamics with different levels of approximate microphysics, with or without MHD. In almost all NS² simulations one finds an accretion disk surrounding a rapidly rotating massive object that eventually collapses to a black hole. An exception is the recent general relativistic simulations of Kiuchi et al. (2010) who find no disks in some configurations. The system lifetime is at least a few dozen milliseconds and possibly longer. The fate of an accretion disk in a BH-NS merger is expected to depend on the mass ratio, the BH spin and the NS compactness. In some cases the disk is very small while in others it is substantial (e.g., Faber et al. 2006; Shibata & Taniguchi 2008).

All simulations find some form of relativistic or sub-relativistic mass ejection. First, matter is ejected as tidal tails during the first stages of the merger. In BH-NS mergers the ejected energy can be very high and its velocity is mildly relativistic. For example Rosswog (2005) find 0.5 c ejecta with $\sim 10^{52}$ erg, where c is the light speed. In a NS² mergers a lower, but yet significant, amount of energy can be ejected (e.g., Rosswog et al. 1999 find $\sim 10^{51}$ erg) at a lower velocities of 0.1 – 0.2 c . This mass ejection is expected also if no significant disk is formed. Disk formation leads to several additional outflow sources. First, neutrino

heating drives a wind from the disk surface (e.g., Levinson 2006; Metzger et al. 2008; Dessart et al. 2009). The energy in this wind is substantial with predictions ranging between 10^{49} erg and 10^{51} erg for $0.01\text{--}0.1\text{ M}_\odot$ disk. The outflow velocity is $\sim 0.1\text{--}0.2\text{ c}$ from the outskirts of the disk and it is increasing, possibly up to relativistic velocities, for wind that is ejected from close to the central object. The mass ejection becomes even stronger when neutrino heating shuts-off and the wind is driven by viscous heating and by He-Synthesis (Lee et al. 2009; Metzger et al. 2009), leading to an ejection of $20\text{--}50\%$ of the initial disk mass at $0.1\text{--}0.2\text{ c}$. Additional energy source is neutrino-antineutrino annihilation above the disk, which can deposit up to $\sim 10^{49}$ erg, into an amount of mass that is not well constrained, leading possibly to a relativistic outflow. Finally, more speculative, but yet very plausible, source of outflow are EM processes that tap the rotational energy of the central object, such as the Blandford-Znajek Mechanism (Blandford & Znajek 1977). These are likely to produce relativistic outflows with an energy that can be as high as 10^{52} erg, and are the most probable engines of short GRBs, if those are produced by compact binary mergers.

The conclusion is that a significant mass and energy ejection is a prediction of almost all compact binary merger modelings. In NS² mergers an ejection of $\gtrsim 10^{50}$ erg at $0.1\text{--}0.2\text{ c}$ is a fairly robust prediction. Faster ejecta (relativistic or mildly relativistic) with energy $\gtrsim 10^{49}$ is also quite likely from inner parts of the $0.01\text{--}0.1\text{ M}_\odot$ disk that is typically found in simulations. The outflow from BH-NS mergers was explored only by a few authors, but it is also seems to be significant and potentially even more energetic and at faster velocities than the outflow from NS² mergers.

3. The radio signal from outflow-ISM interaction

Consider a spherical outflow with an energy E and an initial Lorentz factor Γ_0 , with a corresponding velocity $c\beta_0$, that propagates into a constant density, n , medium. If the outflow is not ultra relativistic, i.e., $\Gamma_0 - 1 \lesssim 1$ it propagates at a constant velocity until, at t_{dec} , it reaches radius R_{dec} , where it collects a comparable mass to its own:

$$R_{dec} = \left(\frac{3E}{4\pi n m_p c^2 \beta_0^2} \right)^{1/3} \approx 10^{17} \text{ cm } E_{49}^{1/3} n^{-1/3} \beta_0^{-2/3}, \quad (1)$$

and

$$t_{dec} = \frac{R_{dec}}{c\beta_0} \approx 30 \text{ day } E_{49}^{1/3} n^{-1/3} \beta_0^{-5/3}, \quad (2)$$

where we approximate $\Gamma_0 - 1 \approx \beta_0^2$ and ignore relativistic effects. Here and in the following, unless stated otherwise, q_x denotes the value of $q/10^x$ in c.g.s. units. At a radius $R > R_{dec}$

the flow decelerates assuming the Sedov-Taylor self-similar solution, so the outflow velocity can be approximated as:

$$\beta \approx \beta_0 \begin{cases} 1 & R \leq R_{dec} , \\ (R/R_{dec})^{-3/2} & R \geq R_{dec} . \end{cases} \quad (3)$$

If the outflow is collimated, highly relativistic and points away from a generic observer, as will typically happen if the mergers produce short GRBs, the emission during the relativistic phase will be suppressed by relativistic beaming. Observable emission is produced only once the external shock decelerates to mildly relativistic velocities and the blast-wave becomes quasi spherical. This takes place when $\Gamma \approx 2$ namely at $R_{dec}(\beta_0 = 1)$. From this radius the hydrodynamics and the radiation become comparable to that of a spherical outflow with an initial Lorentz factor $\Gamma_0 \approx 2$. This behavior is the source of the late radio GRB orphan afterglows (Rhoads 1997; Levinson et al. 2002). Our calculations are therefore applicable for the detectability of mildly and non-relativistic outflows as well as for radio orphan GRB afterglows.

Emission from Newtonian and mildly relativistic shocks is observed in radio SNe and late phases of GRB afterglows. These observations are well explained by a theoretical model involving synchrotron emission of shock accelerated electrons in an amplified magnetic field. The success of this model in explaining the detailed observations of radio Ib/c SNe (e.g., Chevalier 1998; Soderberg et al. 2005; Chevalier & Fransson 2006) allows us to employ the same microphysics here. Energy considerations show that both the electrons and the magnetic field carry significant fractions of the total internal energy of the shocked gas, $\epsilon_e \approx \epsilon_B \sim 0.1$. These values are consistent with those inferred from late radio afterglows of long GRBs (e.g., Frail et al. 2000, 2005). The observed spectra indicate that the distribution of the accelerated electrons Lorentz factor, γ , is a power-law $dN/d\gamma \propto \gamma^{-p}$ at $\gamma > \gamma_m$ where $p \approx 2.1 - 2.5$ in mildly relativistic shocks (e.g., the radio emission from GRB associated SNe and late GRB afterglows) and $p \approx 2.5 - 3$ in Newtonian shocks (as seen in typical radio SNe; Chevalier 1998, and references therein). The value of γ_m is not observed directly but it can be calculated based on the total energy of the accelerated electrons, $\gamma_m = \frac{p-2}{p-1} \frac{m_p}{m_e} \epsilon_e \beta^2$

The radio spectrum generated by the shock is determined by two characteristic frequencies². One is

$$\nu_m \approx 1 \text{ GHz } n^{1/2} \epsilon_{B,-1}^{1/2} \epsilon_{e,-1}^2 \beta^5, \quad (4)$$

the typical synchrotron frequency of electrons with the typical (also minimal) Lorentz factor γ_m . The other is ν_a , the synchrotron self-absorption frequency. We show below that since

²The cooling frequency is irrelevant in the radio.

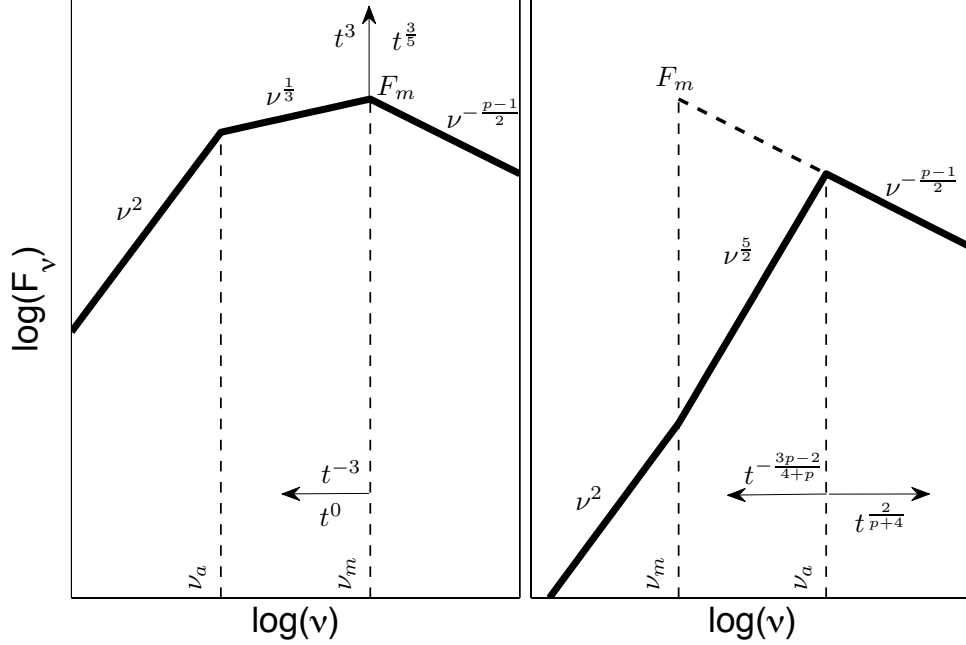


Fig. 1.— A schematic sketch of the two possible spectra and the evolution of the characteristic flux, F_m , and frequencies, ν_a and ν_m . The arrows show the temporal evolution of the characteristic values. The temporal dependence before t_{dec} is noted below/to the left of the arrows while the temporal dependence after t_{dec} is noted above/to the right of the arrows. Note that the evolution of ν_m and F_m , marked only in the left spectrum, is relevant for both spectra. The evolution of ν_a , marked only in the right spectrum, is correct only when $\nu_m < \nu_a$ and is therefore relevant only in that spectrum.

we are interested at the maximal flux at a given observed frequency, ν_a may play a role only if it is larger than ν_m . Its value in that case is

$$\nu_a(> \nu_m) \approx 1 \text{ GHz } R_{17}^{\frac{2}{p+4}} n^{\frac{6+p}{2(p+4)}} \epsilon_{B,-1}^{\frac{2+p}{2(p+4)}} \epsilon_{e,-1}^{\frac{2(p-1)}{p+4}} \beta^{\frac{5p-2}{(p+4)}}. \quad (5)$$

Figure 1 illustrates the two possible spectra, depending on the order of ν_a and ν_m . The flux at any frequency can be found using these spectra and the unabsorbed synchrotron flux at ν_m :

$$F_m \approx 0.5 \text{ mJy } R_{17}^3 n^{3/2} \epsilon_{B,-1}^{1/2} \beta d_{27}^{-2}, \quad (6)$$

where d is the distance to the source (we neglect any cosmological effects). Note that this is the real flux at ν_m only if $\nu_a < \nu_m$ (see figure 1).

As long as the shock is moving with a constant velocity i.e., at $t < t_{dec}$, the flux across the whole spectrum increases (see equations 4-6). The flux evolution at later times depends on the spectrum at t_{dec} , namely on

$$\nu_{m,dec} \equiv \nu_m(t_{dec}) \approx 1 \text{ GHz } n^{1/2} \epsilon_{B,-1}^{1/2} \epsilon_{e,-1}^2 \beta_0^5, \quad (7)$$

and if $\nu_{a,dec} > \nu_{m,dec}$ then possibly on

$$\nu_{a,dec} \equiv \nu_a(t_{dec}) \approx 1 \text{ GHz } E_{49}^{\frac{2}{3(4+p)}} n^{\frac{14+3p}{6(4+p)}} \epsilon_{B,-1}^{\frac{2+p}{2(4+p)}} \epsilon_{e,-1}^{\frac{2(p-1)}{4+p}} \beta_0^{\frac{15p-10}{3(4+p)}}. \quad (8)$$

The flux at that time can be found using the unabsorbed synchrotron flux at $\nu_{m,dec}$:

$$F_{m,dec} \approx 0.5 \text{ mJy } E_{49} n^{1/2} \epsilon_{B,-1}^{1/2} \beta_0^{-1} d_{27}^{-2}. \quad (9)$$

Consider now a given observed frequency ν_{obs} . We are interested at the light curve near the peak flux at this frequency. There are three possible types of light curves near the peak corresponding to: (i) $\nu_{m,dec}, \nu_{a,dec} < \nu_{obs}$, (ii) $\nu_{eq} < \nu_{obs} < \nu_{m,dec}$ and (iii) $\nu_{obs} < \nu_{eq}, \nu_{a,dec}$. Where we define

$$\nu_{eq} = 1 \text{ GHz } E_{49}^{1/7} n^{4/7} \epsilon_{B,-1}^{2/7} \epsilon_{e,-1}^{-1/7} \quad (10)$$

as the frequency at which³ $\nu_m = \nu_a$. In figure 2 we show a schematic sketch of the time evolution of ν_a and ν_m and the corresponding ranges of ν_{obs} in which each of the cases is observed.

To estimate the time and value of the peak flux we recall, that at all frequencies the flux increases until t_{dec} . In case (i), $\nu_{m,dec}, \nu_{a,dec} < \nu_{obs}$, the deceleration time, t_{dec} , is also the time of the peak. The reason is that while F_m increases, ν_m decreases fast enough so that $F_{\nu_{obs}}$ decreases after t_{dec} . Note that in that case ν_a plays no role since it decreases after deceleration. Overall, in this case the flux peaks at t_{dec} and $F_{\nu_{obs},peak} = F_{m,dec}(\nu_{obs}/\nu_{m,dec})^{-(p-1)/2}$.

In the two other cases, (ii) and (iii), $\nu_{obs} < \nu_{m,dec}$ and/or $\nu_{obs} < \nu_{a,dec}$ and the flux keeps rising at $t > t_{dec}$ until $\nu_{obs} = \nu_m(t)$ or $\nu_{obs} = \nu_a(t)$, whichever comes last. To find out which one of the two frequencies is it, we compare ν_{obs} with ν_{eq} . At $t > t_{dec}$, ν_m decreases faster than ν_a . Therefore in case (ii) where $\nu_{eq} < \nu_{obs}$, the last frequency to cross ν_{obs} is ν_m and the peak flux is observed when $\nu_{obs} = \nu_m(t)$. In case (iii) where $\nu_{obs} < \nu_{eq}$, and the last frequency to cross ν_{obs} is ν_a and the peak flux is observed when $\nu_{obs} = \nu_a(t)$. Now, it is straight forward to calculate the peak flux, $F_{\nu_{obs},peak}$ and the time that it is observed, t_{peak} ,

³Note that if $\nu_{m,dec} < \nu_{a,dec}$ this equality will never take place. In that case ν_{eq} is the frequency at which this equality would have happened if Γ_0 would have been large enough (see figure 2)

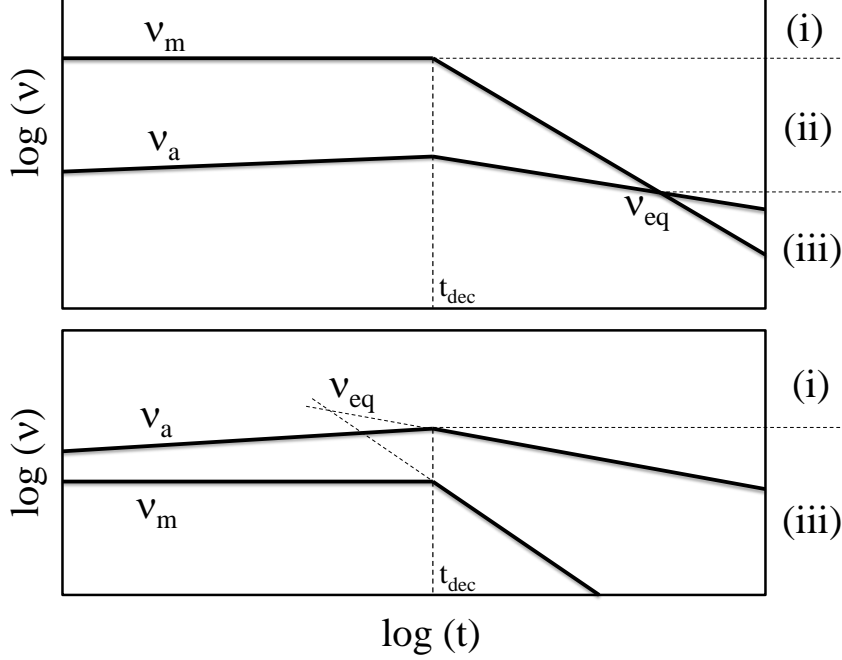


Fig. 2.— A schematic sketch of the time evolution of ν_a and ν_m in two cases, $\nu_{a,dec} < \nu_{m,dec}$ (top) and $\nu_{a,dec} > \nu_{m,dec}$ (bottom). Also marked is the value of ν_{eq} . The vertical dashed line marks t_{dec} . The ranges of ν_{obs} at which each of the cases is observed is separated by horizontal dashed lines and marked on the right. Note that in the bottom panel ν_m and ν_a are not crossing each other at $t > t_{dec}$ and only two types of light curves, cases (i) and (iii), can be observed.

for different frequencies. It is also straight forward to calculate the flux temporal evolution prior and after t_{dec} using equations 4-6 and the relation $t \propto R$ which holds at $t < t_{dec}$ and $\beta \propto t^{-3/5}$ at $t > t_{dec}$. The peak fluxes, the times of the peak and the temporal evolution of the three different cases are summarized in table 1. The overall different light curves are depicted in Fig. 3

The most sensitive radio facilities are at frequencies of 1.4 GHz and higher. Equations 7 and 8 imply that in this frequency range, for most realistic scenarios, it is a case (i) light curve, i.e., $\nu_{a,dec}, \nu_{m,dec} < \nu_{obs}$. Therefore, a Newtonian and mildly relativistic outflows as well as relativistic GRB orphan afterglows peak at t_{dec} with:

$$F_{\nu_{obs},peak}(\nu_{a,dec}, \nu_{m,dec} < \nu_{obs}) \approx 0.3 \text{ mJy } E_{49} n^{\frac{p+1}{4}} \epsilon_{B,-1}^{\frac{p+1}{4}} \epsilon_{e,-1}^{p-1} \beta_0^{\frac{5p-7}{2}} d_{27}^{-2} \left(\frac{\nu_{obs}}{1.4 \text{ GHz}} \right)^{-\frac{p-1}{2}}. \quad (11)$$

The regime of $F_{\nu_{obs},peak}$ at lower radio frequencies ($< 1 \text{ GHz}$) depends on the various

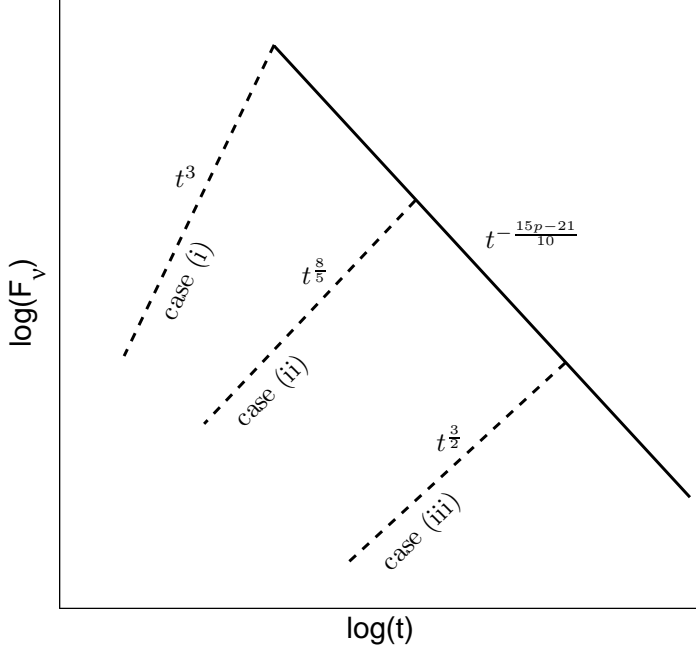


Fig. 3.— Schematic light curves of the three cases. The rising phase, marked in dashed line for each of the the phases, is that of the last temporal power law segment before the peak. After the peak all cases show the same power-law decay.

parameters. If the outflow is Newtonian or the density is low or the energy is low then $\nu_{a,dec}, \nu_{m,dec} < 100$ MHz and equation 11 is applicable. Otherwise low radio frequencies are in regime (iii), i.e., $\nu_{obs} < \nu_{eq}, \nu_{a,dec}$. The flux peaks in this case at

$$t_{peak}(\nu_{obs} < \nu_{eq}, \nu_{a,dec}) \approx 200 \text{ day } E_{49}^{\frac{5}{11}} n^{\frac{7}{22}} \epsilon_{B,-1}^{\frac{9}{22}} \epsilon_{e,-1}^{\frac{6}{11}} \left(\frac{\nu_{obs}}{150 \text{ MHz}} \right)^{\frac{13}{11}}, \quad (12)$$

Regime	$F_{\nu_{obs},peak}/F_{m,dec}$	t_{peak}/t_{dec}	$F_{\nu_{obs}}^\dagger$ $t < t_{peak}$	$F_{\nu_{obs}}$ $t_{peak} < t$
$\nu_{m,dec}, \nu_{a,dec} < \nu_{obs}$	$(\nu_{obs}/\nu_{m,dec})^{-\frac{p-1}{2}}$	1	$\propto t^3$	$\propto t^{-\frac{15p-21}{10}}$
$\nu_{eq} < \nu_{obs} < \nu_{m,dec}$	$(\nu_{obs}/\nu_{m,dec})^{-1/5}$	$(\nu_{obs}/\nu_{m,dec})^{-1/3}$	$\propto t^{\frac{8}{5}}$	$\propto t^{-\frac{15p-21}{10}}$
$\nu_{obs} < \nu_{eq}, \nu_{a,dec}$	$\nu_{m,dec}^{\frac{p-1}{2}} \nu_{a,dec}^{-\frac{3(p+4)(5p-7)}{10(3p-2)}} \nu_{obs}^{\frac{(32p-47)}{5(3p-2)}}$	$(\nu_{obs}/\nu_{a,dec})^{-\frac{4+p}{3p-2}}$	$\propto t^{\frac{3}{2}}$	$\propto t^{-\frac{15p-21}{10}}$

Table 1: The observed flux before and after t_{peak} in the three different regimes.

† The temporal evolution only during the last power-law segment before t_{peak} . At earlier times the temporal evolution may be different.

with

$$F_{\nu_{obs},peak}(\nu_{obs} < \nu_{eq}, \nu_{a,dec}) \approx 50 \mu\text{Jy} E_{49}^{\frac{4}{5}} n^{\frac{1}{5}} \epsilon_B^{\frac{1}{5}} \epsilon_{e,-1}^{\frac{3}{5}} d_{27}^{-2} \left(\frac{\nu_{obs}}{150 \text{ MHz}} \right)^{\frac{6}{5}}. \quad (13)$$

In the last two equations we used $p = 2.5$ (other p values in the range 2.1-3 yield slightly different numerical factors and power laws).

To date, the best observed signal from a mildly relativistic blast waves is the radio emission that follows GRB associated SNe. The main difference is that in these cases the circum burst medium is typically a wind (i.e., $n \propto R^{-2}$) and therefore the density at early times is much larger then in the ISM and self absorption plays the main role in determining the light curve. A good example for comparison of equation 11 with observations is the light curve of SN 1998bw. This light curve is observed at several frequencies at many epochs, enabling a detailed modeling that results in tight constraints of the blast wave and microphysical parameters. Li & Chevalier (1999) find that at the time of the peak at 1.4 GHz, about 40 days after the SN, taking $\epsilon_e = \epsilon_B = 0.1$, the energy in the blast wave is $\sim 10^{49}$ erg, its Lorentz factor is ~ 2 and the external density at the shock radius is $n \sim 1 \text{ cm}^{-3}$. The peak is observed when $\nu_m, \nu_a \leq \nu_{obs}$ and it depends only on these parameters (it is only weakly sensitive to the density profile). Therefore, equation 11 is applicable in that case. Indeed, plugging these numbers into equation 11 we obtain a flux of 20 mJy at the distance of SN 1998bw (40 Mpc), compared to the observed flux of 30 mJy. This is not surprising given that the model we use is based on that of radio SNe.

In the discussion above we considered an outflow with a characteristic energy and velocity. However a compact binary merger may produce an outflow with an energy dependent velocity, e.g., $E(\Gamma_0) \propto (\Gamma_0 - 1)^{-\eta}$. If we consider a case (i) signal ($\nu_{m,dec}, \nu_{a,dec} < \nu_{obs}$; e.g., above 1 GHz) then we find $F_{\nu_{obs},peak} \propto E(\Gamma_0 - 1)^{(5p-7)/4} \propto (\Gamma_0 - 1)^{(5p-7-4\eta)/4}$. Therefore if $\eta < \frac{5p-7}{4} \approx 1.5$ the flux is dominated by the mildly relativistic ejecta, assuming that the relativistic part of the outflow is not pointing towards the observer. Otherwise the flux is dominated by the slowest ejecta.

4. Detection, identification and possible candidates

4.1. detectability

For canonical parameters the strongest signal is expected around 1.4 GHz, conveniently where the sensitivity of radio telescopes is high. If the signal peaks at lower frequencies it decreases from the peak as $\nu^{-(p-1)/2}$. Since 1.4 GHz receivers are ten times more sensitive than lower frequency ones they are still more likely to detect a signal even in this case. Therefore, 1.4 GHz is the optimal frequency to look for radio remnants of compact binary mergers and we therefore consider here the detectability at a 1.4 GHz survey.

The number of events in a single whole sky snapshot is $N_{all-sky} = \mathcal{R}V\Delta t$, where V is the detectable volume at the survey flux limit F_{lim} , Δt is the time that the flux is above the detection limit and \mathcal{R} is the event rate. Since at 1.4 GHz the relevant light curve is case (i) (see §3) we use equations 2 and 11, and the approximation $\Delta t \approx t_{dec}$, to find that the number of radio coalescence remnants in a single 1.4 GHz whole sky snapshot is

$$N_{all-sky}(1.4 \text{ GHz}) \approx 20E_{49}^{11/6} n^{\frac{9p+1}{24}} \epsilon_{B,-1}^{\frac{3(p+1)}{8}} \epsilon_{e,-1}^{\frac{3(p-1)}{2}} \beta_0^{\frac{45p-83}{12}} \mathcal{R}_{300} F_{lim,-1}^{-3/2}. \quad (14)$$

Where $F_{lim,-1} = F_{lim}/0.1 \text{ mJy}$ and \mathcal{R}_{300} is the merger rate in units of $300 \text{ Gpc}^{-3} \text{ yr}^{-1}$.

Since the microphysical parameters are reasonably constrained by radio SNe, the main uncertainty in the signal detectability is the blast-wave properties and the circum-merger density. The latter is expected to vary significantly between different merger events, dropping down to $n \sim 10^{-6} \text{ cm}^{-3}$ for mergers that take place outside of their host galaxies. However, the observed Galactic double-NS population reveals that a significant fraction of compact binary mergers (at least NS²) take place in the disks of Milky-way-like galaxies where $n \sim 1 \text{ cm}^{-3}$.

As discussed in §2 there is a good chance that NS² mergers eject mildly relativistic outflows with $E \gtrsim 10^{49} \text{ erg}$. In that case the EM counterparts of these GW sources are detectable by current facilities. A deep radio survey that covers a significant fraction of the sky will most likely detect their radio remnants to a distance of $\sim 300 \text{ Mpc}$. These will appear as transients, varying on a several weeks time scale, with an optically thin spectrum at $\nu \gtrsim 1 \text{ GHz}$ at all time. The radio remnants will be identified in random places within their host galaxies, which should be easily detectable at that distance. It will not be accompanied by any optical counterpart with similar variability time scales. Given a GW trigger with localization of $10 - 100 \text{ deg}^2$, a deep search of the error box will detect a remnant in cases that the surrounding density is not very low.

NS² mergers are also expected to eject energetic, $E \gtrsim 10^{50} \text{ erg}$, outflow at lower veloci-

ties, $\beta_0 = 0.1 - 0.2$. The detectability is very sensitive to the velocity, $N \propto \beta_0^{2.5}$ for $p = 2.5$, and to the energy, $N \propto E^{11/6}$. Therefore, even if there is no mildly relativistic component to the outflow, the number of detectable remnants that are dominated by slow moving ejecta is expected to be significant. For example, assuming that an energy of 10^{50} erg is ejected at $\beta_0 = 0.2$ we expect $N_{all-sky} \sim 10\mathcal{R}_{300}F_{lim,-1}^{-3/2}$. The variability time scale of these transients is expected to be ~ 3 yr. If the velocity is instead $0.1c$ the number of events drops by an order of magnitude and the variability timescale increases to ~ 10 yr. These time scales increase the difficulty in the identification of the remnants as transients, and require a long term survey. The spectrum of these transients will be optically thin also at low frequencies (~ 100 MHz). Other characteristics of these transients (e.g., location within the host) are expected to be similar to that of a mildly relativistic outflow. A GW triggered search increases of course the probability to find a remnant and a $> 10^{50}$ erg outflow can be detected up to 300 Mpc even if its velocity is $\sim 0.1c$.

The detectability of BH-NS mergers is much harder to predict. First due to their virtually unconstrained rate and second since the properties of the outflow are less certain. The latter can be significantly improved by current and future merger simulations that put focus on the ejected mass. In any case the potential of these mergers to throw out a considerable amount of energy, $\sim 10^{51}$ erg, at mildly relativistic velocities can make them detectable to their GW detection horizon, which is much further than the NS² horizon.

Finally, if compact binary mergers launch also collimated ultra-relativistic outflows, and produce short GRB, then orphan short GRB afterglows are also part of the post merger EM signal. The detectability of radio orphan afterglows can be estimated based on observations of short GRBs and is independent of whether they are produced by mergers or not. We discuss their detectability in the next subsection. All together, the range of the current predictions is rather large, but with most parameters we expect detectable radio signals. Some of the new generation radio telescopes have large fields of view (e.g., ASKAP⁴ with 30 deg^2 and Apertif with 8 deg^2 ; Oosterloo et al. 2010) and improved sensitivities, making them ideal for large scale sub-mJy blind survey. The EVLA, which has a smaller field of view but a remarkable sensitivity, is the best facility for GW triggered search. It is also currently the fastest radio-survey instrument and it can carry-out a sub-mJy blind survey. All these observatories have a very good chance to detect compact binary merger remnants in dedicated blind searches. In fact with very reasonable parameters (e.g., $E \sim 10^{50}$ erg of mildly relativistic ejecta) a sub-mJy whole sky survey can detect thousands of binary-merger radio remnants.

⁴<http://www.atnf.csiro.au/projects/askap/technology.html>

4.2. Radio orphan afterglows of short GRBs

Short GRB outflow begins highly relativistic and probably highly beamed. Eventually it slows down (see §3) and become detectable from all directions. Therefore, the rate estimate equation 14 is also applicable for radio orphan afterglows when $\beta_0 = 1$. However some of the parameters in equation 14 are not directly observable. The observed quantities are isotropic equivalent γ -ray energy, $E_{\gamma,iso}$, and the rate of bursts that point to the observer \mathcal{R}_{obs}^{SHB} , while equation 14 depends on $E = E_{iso}f_b$ and $\mathcal{R}^{SHB} = \mathcal{R}_{obs}^{SHB}f_b^{-1}$, where $f_b < 1$ is the fraction of the 4π steradian covered by the jet and E_{iso} is the isotropic equivalent energy in the afterglow blast wave. X-ray observations indicate that γ -ray emission in short GRBs is very efficient and that in general $E_{iso} \sim E_{\gamma,iso}$ (Nakar 2007). We assume that this is the case in the following discussion.

$E_{\gamma,iso}$ of short GRBs ranges at least over four orders of magnitude ($10^{49} - 10^{53}$ erg). The rate of observed short GRBs is dominated by 10^{49} erg bursts, and the luminosity function can be well approximated by a power-law, at least in the range $\sim 10^{49} - 10^{51}$ erg, such that $\mathcal{R}_{obs}^{SHB}(E) \sim 10E_{49}^{-\alpha} \text{ Gpc}^{-3} \text{ yr}^{-1}$ where $\alpha \approx 0.5 - 1$ (Nakar et al. 2006; Guetta & Piran 2006). Plugging these into equation 14 we obtain

$$N_{all-sky}^{SHB}(1.4 \text{ GHz}) \approx 1f_b^{5/6} E_{49}^{\frac{11}{6}-\alpha} n^{\frac{9p+1}{24}} \epsilon_{B,-1}^{\frac{3(p+1)}{8}} \epsilon_{e,-1}^{\frac{3(p-1)}{2}} F_{lim,-1}^{-3/2}. \quad (15)$$

This equation is similar to equation 9 of Levinson et al. (2002), with the observed luminosity function already folded in.

Narrower beamed bursts (with lower f_b) are more numerous and they produce less total energy per burst. The positive dependence of equation 15 on f_b implies that overall the lower energy is “winning” over the increased rate, and the detectability of narrower bursts is lower. Using, equation 15 we can put a robust upper-limit on the orphans rate since all the parameters are rather well constraint by observations, with the exception of f_b which is < 1 by definition. Therefore, assuming that short GRBs are beamed, the detection of the common $\sim 10^{49}$ erg bursts in a blind survey, even with next generation radio facilities, is unlikely (Nakar 2007). However, brighter events should be detectable. If the beaming is energy independent, detectability increases with the burst energy. The luminosity function possibly breaks around 10^{51} erg, in which case the orphans number is dominated by 10^{51} erg bursts. For $f_b^{-1} = 30$ we expect, from these bursts ~ 10 orphan afterglows at a 0.1 mJy in a single 1.4 GHz whole sky snapshot.

So far we discussed detectability in a blind survey. A followup dedicated search would be, of course, more sensitive. If compact binary mergers produce short GRBs than the energy of most GW detected bursts will be faint with $E_{\gamma,iso} \sim 10^{49}$ erg. The chance to detect their orphan afterglows again depended on their total energy and thus on f_b . Equation 11 shows

that if $f_b^{-1} = 30$ then detection should be difficult but possible in a dedicated search mode. Note that since the energy of the burst is low, the radio emission will evolve quickly, reaching a peak and decaying on a week time scale, so a prompt and rather deep search will be needed.

4.3. Possible candidates of compact binary merger remnants

Bower et al. (2007) carried out a 5 GHz survey looking for transients on timescales of a week to a year. The survey sensitivity for transients with variability scale < 7 day is 0.37 mJy with an effective area of $\approx 10 \text{ deg}^2$. Events with variability time scale of two months were surveyed at sensitivity of 0.2 mJy with an effective area of $\approx 2 \text{ deg}^2$.

Bower et al. (2007) report the detection of 10 transients. The most interesting of those, in our context, is RT 19870422, which has a variability time scale of two months. It is found within a star forming galaxy at a distance of 1.05 Gpc, but at a significant offset from the host nucleus. Its luminosity and time scale are those expected from a $\sim 10^{50}$ erg mildly relativistic outflow that propagates in the ISM. It is, therefore, a prime candidate for a compact binary merger radio remnant. Based on this single event Bower et al. (2007) infer a best estimate rate of $4 \times 10^3 \text{ Gpc}^{-3} \text{ yr}^{-1}$ for RT 19870422-like events. Taking a 2σ Poisson error, the best estimate translates to a range of $80 - 20,000 \text{ Gpc}^{-3} \text{ yr}^{-1}$, fully consistent with the estimates of compact binary mergers. If this is indeed a merger remnant then, since for optically thin spectrum the fluxes at 1.4 GHz and 5 GHz are not very different, a sub-mJy 1.4 GHz whole sky survey would detect hundreds to thousands of radio remnants. Bower et al. (2007) suggested that this transient is a radio SNe similar to SN 1998bw, but brighter. This is certainly a viable possibility, however, if true then this radio SN is brighter by an order of magnitude than the brightest radio SN ever observed before. Unfortunately, lacking optical search for a SN or a multi-wavelength measurement that determines the transient spectrum, it is impossible to rule out any of the two possibilities.

An additional interesting candidate is RT 19840613. It is variable on less than 7 days and it has a host galaxy at a distance of 140 Mpc. Even assuming a variability time scale of 7 days it is marginal as a merger remnant candidate. Assuming 7 days variability Bower et al. (2007) find a rate of $(0.6 - 150) \times 10^4 \text{ Gpc}^{-3} \text{ yr}^{-1}$, which is again only marginally consistent with current estimates of compact binary merger rates. Therefore, while this may be a merger remnant it is not a very promising candidate. Bower et al. (2007) suggest that this is also a SN 1998bw-like event. While this possibility cannot be ruled out, the inferred rate is at least an order of magnitude larger than that of 98bw-like events (note that radio SNe as bright as SN 1998bw are very rare compared to typical radio SNe). The additional 8 events detected by Bower et al. (2007) have no clear host galaxies and are therefore probably

not merger remnants.

4.4. Identification and contamination

A key issue with the detection of compact binary merger remnants in blind surveys is their identification. Ofek et al. (2011) present a census of the transient radio sky. Luckily the transient radio sky at 1.4 GHz are relatively quiet. The main contamination source are radio active Galactic nuclei (AGNs), however their persistent emission is typically detectable in other wavelength and/or deeper radio observations. Moreover, the signal from a compact binary merger is expected to be located within its host galaxy (otherwise the density is too low), but away from its center. The host and the burst location within it, should be easily detectable at the relevant distances.

The only known, and guaranteed, transient 1.4 GHz source with similar properties are radio SNe. Among these typical radio SNe are the most abundant. Transient search over 1/17 of the sky with $F_{lim} = 6$ mJy at 1.4GHz (Levinson et al. 2002; Gal-Yam et al. 2006; Ofek et al. 2010) finds one radio SN. This rate translates to $10^3 - 10^4$ SNe in a whole sky $F_{lim} = 0.1$ mJy survey. These contaminants can be filtered in three ways. First, by detection of the SN optical light. However, the optical signal may be missed if it is heavily extinguished, and given the large number of radio SNe, misidentifying even a small fraction of them may render the survey useless for our purpose. The second filter is the optically thick spectrum at high radio frequency (~ 10 GHz) at early times, which is a result of the blast wave propagation in a wind. Thus, a multi-wavelength radio survey can identify radio SNe. The last filter is the luminosity-time scale relation of typical radio SNe that is induced by the outflow velocity (e.g., figure 2 in Chevalier et al. 2006). Type II SN outflows are slow, $\sim 0.01c$, and therefore their radio emission is longer/fainter than that expected for merger remnants. The common type of Ib/c radio SNe is produced by $\sim 0.2c$ blast waves but with much less energy than what we expect from a binary merger outflow, and therefore their radio emission is much fainter. The combination of any two of these filters will hopefully be enough to identify all the typical radio SNe.

Slightly different contaminants are GRB associated SNe. Their outflows is as fast and as energetic as those that we expect from a binary merger and therefore their radio signature is similar in time scales and luminosities. SN1998bw-like events are detectable by a 0.1 mJy survey at 1.4 GHz up to a distance of several hundred Mpc for 40 days and their rate is $40 - 700 \text{ Gpc}^{-3} \text{ yr}^{-1}$ (Soderberg et al. 2006), implying at least several sources at any whole sky snapshot. Here only the first filter (SN optical light) and possibly the second (optically thick spectrum) can be applied. However, given the high optical luminosity of

GRB associated SNe and their relatively low number this should be enough in order to filter them out. These contaminators highlight the importance of a multi-wave length strategy where an optical survey accompany the radio survey to best utilize both surveys detections.

The results of Bower et al. (2007) implies that thousands of sources with properties similar to RT 19870422 are expected in a 5 GHz sub-mJy all sky survey. If these events are optically thick during their whole evolution than these are not merger remnants and they could be easily filtered out. Moreover, in that case their rate in a 1.4 GHz survey should be lower by two orders of magnitude. If these events show a synchrotron optically thin spectrum and no optical counterparts, then they should be abundant also in a 1.4 GHz survey, and their origin is most likely compact binary mergers.

Finally, radio is the place to look for blast waves in tenuous mediums, regardless of their origin. Any source of such explosion, being a binary merger, a GRB or a SN, produces a radio signature. Therefore, all the strong explosions may be detectable is a deep radio survey, this include for example long GRB on-axis and off-axis afterglows and giant flares from extra galactic soft gamma-repeaters. The difference between the radio signatures of the different sources (amplitude, spectrum and time evolution) depends on the blast wave energy and velocity and on the external medium properties. We thus will be able to identify the characteristics of binary mergers outflows. If, however, there is a different source of $\sim 10^{50}$ erg of mildly relativistic outflow that explodes in the ISM it will be indistinguishable from binary mergers (at least not in the radio). Currently we are not aware of any such source, with the exception of long GRBs at the low end of the luminosity function, but these are too rare to contaminate a survey. Any other source of such outflows, if exist, will probably be a part of the family of collapsing/coalescing compact objects.

5. Conclusion

Compact binaries are expected to eject sub-relativistic, mildly relativistic and possibly ultra-relativistic outflows as part of their merger process. We have shown that these outflows will inevitably produce a long lived radio remnant. These are the most robust predictions of an EM counterpart of the merger GW signal. The radio remnant appears weeks to years after the merger and remains bright for a similar time. Therefore, a trigger following a detection of GW signal can wait for a week after the event and no online triggering is needed. In addition the long lasting remnants enable a detection in a blind survey. For mildly relativistic outflows with 10^{49} erg that propagate in the ISM we expect a few weeks radio transients with a 1.4 GHz flux of ~ 0.3 mJy from sources at ~ 300 Mpc, the advanced LIGO-Virgo horizon for NS² mergers. The BH-NS GW horizon is farther, but current numerical simulations suggest

they involve higher energy outflow resulting in a comparable flux. Follow up observations of GW candidate events, at a level of $\sim 10\mu\text{Jy}$ are feasible and are very likely to show a radio transient for either NS^2 merger or BH-NS merger.

We find that the optimal frequency to carry out a search for merger remnants is 1.4 GHz. Assuming a mildly relativistic outflow with 10^{49} erg the canonical NS^2 merger rate of $300 \text{ Gpc}^{-3} \text{ yr}^{-1}$ (and a range of $20 - 2 \times 10^4 \text{ Gpc}^{-3} \text{ yr}^{-1}$) implies a detection of ~ 20 (1-1200 correspondingly) radio NS^2 remnants in a 0.1 mJy all sky survey. This rate depends quadratically on the outflow energy, so a very plausible ejected energy of 10^{50} erg increases the rate by two orders of magnitude, making them detectable even in a survey that covers only a small fraction of the sky or that is at a mJy sensitivity. Therefore carrying out a large field-of-view and sensitive GHz survey by currently available facilities has a great potential to constrain the rate of binary mergers, a piece of information that is of great importance for the design and operation of GW detectors.

Even if mergers do not launch a significant mildly relativistic ejecta they are still expected to produce an energetic ($\gtrsim 10^{50}$ erg) sub-relativistic (0.1-0.2)c outflows. These outflows will also produce radio remnants. These remnants will be fainter, detectable only to a distance of $\sim 100 \text{ Mpc}$ at 0.1 mJy, and will evolve more slowly, on time scales of 3-10 yr. These transients are also detectable at a rate of ~ 10 over the whole sky at 0.1 mJy, although identifying them as transients is harder and it requires a long term survey.

We estimate the detectability of short GRB orphan afterglows, which may also be produced by compact binary mergers if they are launching also ultra-relativistic outflows. These estimates are based on short GRB observations and are therefore indifferent to whether short GRBs are binary mergers or not. The main uncertainty in the rate estimates is the GRB beaming factor. We find that assuming $f_b^{-1} = 30$ there are expected to be about 10 orphan afterglows at a 0.1 mJy in a single 1.4 GHz whole sky snapshot. The duration of these afterglows is several weeks. If binary mergers are short GRBs then a GW triggered event will most likely be of a low energy GRB, $E_{\gamma,iso} \sim 10^{49}$ erg, and a true energy, after beaming correction, that is even lower. The radio orphan afterglow will probably still be detectable in a deep search. However its variability time scale is short, about a week, so the search should be done promptly.

Remarkably, the observed 5 GHz transient RT 19870422, detected by Bower et al. (2007) fits very well our estimates of the typical expected properties of a compact binary merger radio remnant. At a distance of 1 Gpc and a duration of two months this transient is what expected from a mildly relativistic outflow with $\sim 10^{50}$ erg. The rate inferred from this single event is also fully consistent with that of NS^2 mergers. This transient is an excellent candidate to be the first observed radio remnant of a merger. Unfortunately, one can not rule out the

possibility, suggested by Bower et al. (2007), that this is an especially bright radio SN. Note, however, that this interpretation requires a SN brighter by an order of magnitude than any radio SNe previously observed. Simultaneous optical observations or multi-wavelength radio observations could have easily distinguished between the two possibilities. The first could have determined if there was a SN or not. The second could have distinguished between an optically thick radio spectrum expected in radio SNe vs the optically thin spectrum expected in merger remnants at these frequencies at all times. Unfortunately, no such observations were available. However, the rate implied by this even is very high and similar events should be detected in a sub-mJy survey of even a small fraction of the sky. Therefore, the nature of this type of events can be easily probed with current facilities.

Our results show the great potential of 1.4 GHz radio transient observations at the sub-mJy level for the detection of NS² mergers. On the observational side these predictions provide an excellent motivation for carrying out a whole sky sub-mJy survey using the EVLA or other upcoming radio telescopes. The main source of contamination in such surveys would be radio supernova and those could be distinguished from compact binary mergers by their optical signal, spectrum and other characteristic properties.

While it is clear that compact binary mergers produce sub-relativistic to relativistic outflows, details of those outflows are not well determined at present. This is to large extent because of lack of interest rather than because of specific difficulties in analyzing their properties. Our analysis elucidate the importance of a detailed quantitative estimates concerning these outflows, a task that is within the scope of current simulations.

We thank Dale Frail, Shri Kulkarni, Andrew MacFadyen, Eran Ofek and Stephan Rosswog for helpful discussions. This research was supported by an ERC advanced research grant, by the Israeli center for Excellent for High Energy AstroPhysics, by the Israel Science Foundation (grant No. 174/08) and by an IRG grant.

REFERENCES

- Abadie, J., et al. 2010, *Classical and Quantum Gravity*, 27, 173001
- Abbott, B. P., et al. 2009a, *Reports on Progress in Physics*, 72, 076901
- . 2009b, *Phys. Rev. D*, 80, 047101
- Acernese, F., et al. 2008, *Classical and Quantum Gravity*, 25, 114045
- Belczynski, K., Kalogera, V., Rasio, F. A., Taam, R. E., Zezas, A., Bulik, T., Maccarone, T. J., & Ivanova, N. 2008, *ApJS*, 174, 223

- Blandford, R. D., & Znajek, R. L. 1977, MNRAS, 179, 433
- Bower, G. C., Saul, D., Bloom, J. S., Bolatto, A., Filippenko, A. V., Foley, R. J., & Perley, D. 2007, ApJ, 666, 346
- Chevalier, R. A. 1998, ApJ, 499, 810
- Chevalier, R. A., & Fransson, C. 2006, ApJ, 651, 381
- Chevalier, R. A., Fransson, C., & Nymark, T. K. 2006, ApJ, 641, 1029
- Dessart, L., Ott, C. D., Burrows, A., Rosswog, S., & Livne, E. 2009, ApJ, 690, 1681
- Eichler, D., Livio, M., Piran, T., & Schramm, D. N. 1989, Nature, 340, 126
- Faber, J. A., Baumgarte, T. W., Shapiro, S. L., & Taniguchi, K. 2006, ApJ, 641, L93
- Frail, D. A., Soderberg, A. M., Kulkarni, S. R., Berger, E., Yost, S., Fox, D. W., & Harrison, F. A. 2005, ApJ, 619, 994
- Frail, D. A., Waxman, E., & Kulkarni, S. R. 2000, ApJ, 537, 191
- Gal-Yam, A., et al. 2006, ApJ, 639, 331
- Granot, J., & Sari, R. 2002, ApJ, 568, 820
- Grote, H., & the LIGO Scientific Collaboration. 2008, Classical and Quantum Gravity, 25, 114043
- Guetta, D., & Piran, T. 2006, A&A, 453, 823
- Guetta, D., & Stella, L. 2009, A&A, 498, 329
- Hansen, B. M. S., & Lyutikov, M. 2001, MNRAS, 322, 695
- Kalogera, V., et al. 2004a, ApJ, 614, L137
- . 2004b, ApJ, 601, L179
- Kiuchi, K., Sekiguchi, Y., Shibata, M., & Taniguchi, K. 2010, Physical Review Letters, 104, 141101
- Kochanek, C. S., & Piran, T. 1993, ApJ, 417, L17+
- Law, N. M., et al. 2009, PASP, 121, 1395

- Lee, W. H., Ramirez-Ruiz, E., & López-Cámara, D. 2009, *ApJ*, 699, L93
- Levinson, A. 2006, *ApJ*, 648, 510
- Levinson, A., Ofek, E. O., Waxman, E., & Gal-Yam, A. 2002, *ApJ*, 576, 923
- Li, L., & Paczyński, B. 1998, *ApJ*, 507, L59
- Li, Z., & Chevalier, R. A. 1999, *ApJ*, 526, 716
- LSST Science Collaborations et al. 2009, ArXiv e-prints
- Mandel, I., & O’Shaughnessy, R. 2010, *Classical and Quantum Gravity*, 27, 114007
- Metzger, B. D., Piro, A. L., & Quataert, E. 2008, *MNRAS*, 390, 781
- . 2009, *MNRAS*, 396, 304
- Metzger, B. D., et al. 2010, *MNRAS*, 406, 2650
- Moortgat, J., & Kuijpers, J. 2004, *Phys. Rev. D*, 70, 023001
- Nakar, E. 2007, *Phys. Rep.*, 442, 166
- Nakar, E., Gal-Yam, A., & Fox, D. B. 2006, *ApJ*, 650, 281
- Narayan, R., Piran, T., & Shemi, A. 1991, *ApJ*, 379, L17
- Ofek, E. O., Breslauer, B., Gal-Yam, A., Frail, D., Kasliwal, M. M., Kulkarni, S. R., & Waxman, E. 2010, *ApJ*, 711, 517
- Ofek, E. O., Frail, D. A., Breslauer, B., Kulkarni, S. R., Chandra, P., Gal-Yam, A., Kasliwal, M. M., & Gehrels, N. 2011, in preparation
- Oosterloo, T., Verheijen, M., & van Cappellen, W. 2010
- Phinney, E. S. 1991, *ApJ*, 380, L17
- Pshirkov, M. S., & Postnov, K. A. 2010, *Ap&SS*, 330, 13
- Rau, A., et al. 2009, *PASP*, 121, 1334
- Rezzolla, L., Baiotti, L., Giacomazzo, B., Link, D., & Font, J. A. 2010, *Classical and Quantum Gravity*, 27, 114105
- Rhoads, J. E. 1997, *ApJ*, 487, L1+

- Rosswog, S. 2005, *ApJ*, 634, 1202
- Rosswog, S., Davies, M. B., Thielemann, F., & Piran, T. 2000, *A&A*, 360, 171
- Rosswog, S., Liebendörfer, M., Thielemann, F., Davies, M. B., Benz, W., & Piran, T. 1999, *A&A*, 341, 499
- Rosswog, S., & Price, D. 2007, *MNRAS*, 379, 915
- Ruffert, M., & Janka, H. 2001, *A&A*, 380, 544
- Sari, R., Piran, T., & Narayan, R. 1998, *ApJ*, 497, L17+
- Sengupta, A. S., the Ligo Scientific Collaboration, & the Virgo Collaboration. 2010, *Journal of Physics Conference Series*, 228, 012002
- Shibata, M., & Taniguchi, K. 2008, *Phys. Rev. D*, 77, 084015
- Smith, J. R., & LIGO Scientific Collaboration. 2009, *Classical and Quantum Gravity*, 26, 114013
- Soderberg, A. M., Kulkarni, S. R., Berger, E., Chevalier, R. A., Frail, D. A., Fox, D. B., & Walker, R. C. 2005, *ApJ*, 621, 908
- Soderberg, A. M., et al. 2006, *Nature*, 442, 1014
- the LIGO Scientific Collaboration, & the Virgo Collaboration. 2010, *ArXiv e-prints*
- Waxman, E., Kulkarni, S. R., & Frail, D. A. 1998, *ApJ*, 497, 288
- Yamamoto, T., Shibata, M., & Taniguchi, K. 2008, *Phys. Rev. D*, 78, 064054